

# INDUCTIVE HIGH VOLTAGE PULSE GENERATOR BASED ON RESONANCE SYSTEM

Adam Lindblom — Jan Isberg — Hans Bernhoff — Mats Leijon \*

A high voltage pulse generator based on inductive intermediate energy storage has been constructed. The current switching technique used in the generator is based on a resonance system. Opening switches for high currents are generally difficult to construct and the switch used here has proven to turn off 1.8 kA DC-current at a rate of 300 A/ $\mu$ s. The generator is equipped with a step-up transmission line transformer as intermediate magnetic energy storage and the primary and secondary energy storages are capacitive. An LC-resonance circuit is combined with 3 vacuum interrupters in series as an opening switch on the primary side of the transformer. Discharging the capacitor bank into the primary winding of the transformer introduces a 200 Hz sinusoidal oscillation on the primary current. The movable contacts in the vacuum interrupters are operated mechanically and stable arcs are formed as the gaps are opened. As the 200 Hz sinusoidal current reaches its first maximum, the small LC-resonance circuit is triggered and the current achieves a new frequency of 25 kHz. The large amplitude and high frequency generated by the LC-resonance circuit results in a zero crossing of the primary current. As the current crosses zero the arc deionises and the current is switched off. Pulse shaping with a  $2 \times 50$  m Blumlein configuration on the secondary side of the transformer has been investigated. A rise-time of 40 ns and pulse duration of 700 ns were measured for a resistive load. The aim with this pulse generator is to get familiar with the challenges involved in scaling the system to higher performance.

**Key words:** high voltage, pulsed power, transformer, transmission line, vacuum interrupter, current switch

## 1 INTRODUCTION

Generation of high power microwaves puts specific demands on pulse generators, the rise time and pulse length have to be within certain limits. This generator was designed in order to learn how to handle and interrupt large currents. Switching techniques involving large currents are necessary to handle in order to sustain low costs for transformers. This becomes especially important for pulse generators based on intermediate magnetic energy storages. The pulse generator investigated in this article is equipped with primary and secondary capacitive energy storages as shown in Fig. 1. A step-up transformer with an air-core is used as an intermediate energy storage. The opening switch for the pulse generator is based on a triggered resonance circuit in combination with vacuum interrupters. Designing the generator with a resonance circuit in combination with vacuum interrupters allows a repetitive function. The easiest way to interrupt a large current is to use exploding wires, however, exploding wires have drawbacks such as a low repetition rate. The transformer used in this generator is similar to the one tested in [1] and [2]. Both transformers are made from coaxial high voltage transmission lines [3]. The transmission lines are made from cross-linked polyethylene and can withstand a DC-voltage stress of 100 kV/mm [4]. The transmission lines have been used successfully in high voltage rotating machines such as Powerformer<sup>TM</sup> [5] and transformers without oil immersion [6].

## 2 PULSE GENERATOR

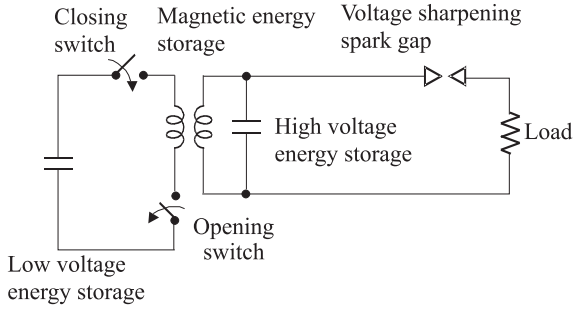
### 2.1 Full scale 500 kV generator

The aim with the investigated scale model in this article is to get familiar with the challenges involved in a full-scale pulse generator. A full-scale generator designed for the performance 500 kV, 50 kA, 20 ns rise time and 1  $\mu$ s pulse duration provides an engineering challenge. The semi-square pulse would contain 25 kJ and the resulting primary energy storage should contain at least 50 kJ considering 50% overall efficiency. Further, using a 1:4 step-up air-core transformer sets the primary current to 3.3 kA considering a 9 mH primary inductance and 1 mF primary capacitor bank. As the primary current is switched off, induction voltages of 125 kV and 500 kV appear on the primary secondary winding, whereas the secondary winding is connected to a 0.2  $\mu$ F pulse forming Blumlein. Semiconductors at reasonable cost and size are not suited as commutators [7], [8], [9] for the vacuum interrupters because the energy transport and induction voltage is too high. A slightly different approach that uses a resonance circuit (instead of semiconductors) combined with vacuum interrupters is explained in section (2.2).

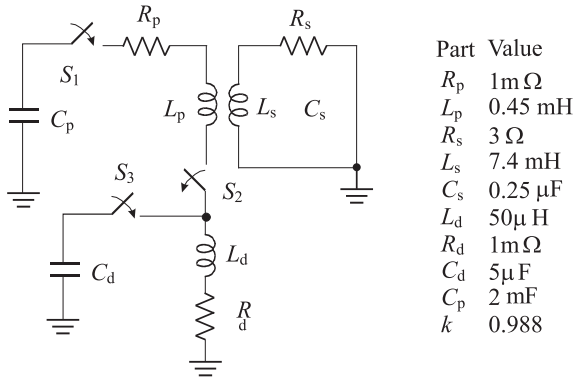
### 2.2 Scale model pulse generator

Figure 2 describes a simplified schematic of the pulse generator where the components  $C_p$ ,  $R_p$ ,  $L_p$  are the primary capacitance, resistance and inductance.  $C_s$ ,  $R_s$ ,  $L_s$

\* Division for Electricity and Lightning Research, Ångströmlaboratoriet, Uppsala University, SE-75121 Uppsala, Sweden. E-mail: Adam.Lindblom@Angstrom.uu.se



**Fig. 1.** Pulse generator using a transformer as an intermediate energy storage. The high voltage energy storage is replaced (section III) with a Blumlein in order to sustain a square load voltage.



**Fig. 2.** a) Pulse generator circuit with a transmission line transformer and a secondary high voltage capacitor  $C_s$ , the resonance circuit consists of  $L_d$ ,  $C_d$  and is used for achieving zero current crossing. b) Table with component values used in the simulation of the simplified circuit.

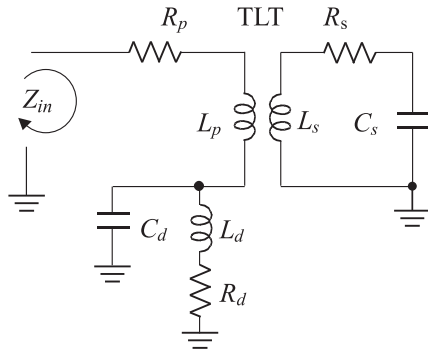


**Fig. 3.** A simplified version of the circuit used in the simulation program [11]

are the secondary capacitance, resistance and inductance.  $C_d$ ,  $R_d$ ,  $L_d$  forms the resonance circuit. The first switch  $S_1$  contains a thyristor and switch  $S_2$  contains 3 vacuum interrupters in series. The movable contact in the vacuum interrupters are operated mechanically with a mean velocity of 7 m/s, the specific velocity of the movable contact allows a full stroke (7 mm) in 1 ms. The last switch  $S_3$  is a triggered 10 kV spark gap.

The operating principle for the pulse generator is illustrated in Fig. 2. The primary capacitive energy storage  $C_p$  is discharged through the primary winding  $L_p$  and

the resonance inductance  $L_d$  by closing switch  $S_1$ . The movable contacts in  $S_2$  are operated shortly after switch  $S_1$  and stable arcs are formed in the vacuum interrupters. When the third switch  $S_3$  is closed at current maximum, the pre-charged energy in capacitor  $C_d$  forms a resonance circuit with the energy stored in inductor  $L_d$ . The current switches from the slow 200 Hz sinusoidal to 25 kHz as resonance occurs. The high  $Q$ -value of the 25 kHz resonance circuit results in zero ampere crosses. As the amplitude of the current passes zero for some microseconds, the arcs are deionised in the vacuum interrupters and the current is effectively switched off. The magnetically stored energy in the transformer is converted to a high voltage across the secondary capacitor  $C_s$  as the current is interrupted. A typical test uses 1.2 kV in the primary capacitor  $C_p$  and 6 kV in the resonance capacitor  $C_d$ .

### 2.3 Input impedance

The input impedance is calculated with the primary capacitor  $C_p$  removed and all switches closed. The transformer is converted into an equivalent reciprocal two-port network [14]. This common procedure is applied because it makes the circuit calculations simple. Figure 3 shows a simplified version of the circuit used in the simulation program [11]. The transformer model used in the electric circuit simulations was previously presented in [1] and has a distributed inductance, capacitance and resistance. The lumped circuit element [9], [10] approach was used in the electric circuit model. The input impedance is calculated with the switches closed and the primary capacitor  $C_p$  removed. The transformer network is assumed reciprocal and the T-model [14] is used. The input impedance is calculated and the result becomes

$$Z_{in}(j\omega) = R_p + j\omega L_p + \frac{R_d + j\omega L_d}{1 - \omega^2 L_d C_d + j\omega R_d C_d} + j \frac{\omega^3 k^2 L_p L_s C_s}{1 - \omega^2 L_s C_s + j\omega R_s C_s}, \quad (1)$$

where  $k$  is the coupling factor of the transformer and  $\omega$  is the angular frequency. The real roots of the modulus of eq. (1) can be solved analytically with the resistance set to zero. The easiest way to get an overview of the circuit impedance is to run the circuit in the electric circuit simulation program. However, the analytical solution gives an overview of the components that significantly affect the impedance. Figure 4 shows the modulus of the input impedance with switch  $S_3$  (Fig. 2) closed and opened.

## 3 GENERATOR DESIGN

### 3.1 Opening switch

The opening switch  $S_2$  has three vacuum interrupters in series resulting in a higher electrical insulating capability [15]. The electric circuit model of the vacuum interrupter in switch  $S_2$  is shown in Fig. 5 and contains a

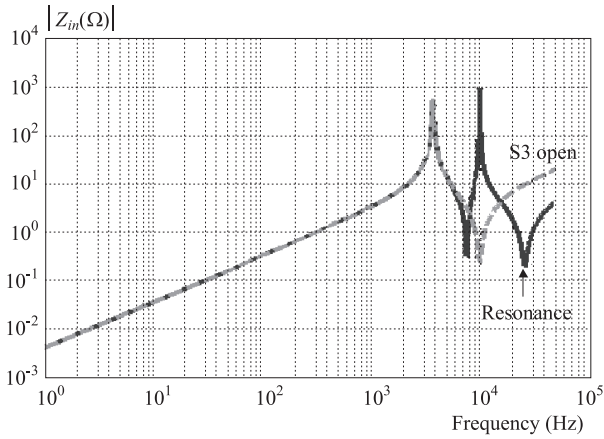


**Fig. 4.** The impedance changes as switch  $S_3$  is operated and resonance occurs at 25 kHz.

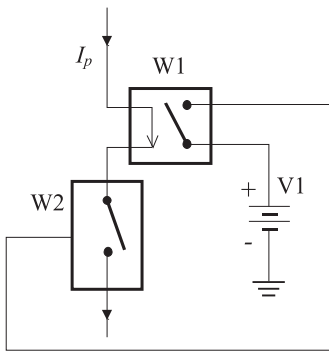


**Fig. 5.** Spice model for the opening switch, the switch  $W_2$  is opened as switch  $W_1$  senses zero current.

current switch  $W_1$ . The current switch  $W_1$  outputs the voltage  $V_1$  as the current  $I_p$  passes zero, in turn this voltage control the switch  $W_2$  and the opening procedure is established. The circuit shown in Fig. 5 is a rough simulation model of the vacuum interrupters that is used in the experimental setup. A stable arc occurs in each vacuum interrupter if the movable contact is operated during current flow. The conducting arcs are modelled as an inner resistance in switch  $W_1$  and the extinguishing of the arcs are modelled by switch  $W_2$  that has the logic function on or off.

Switch  $S_3$  (shown in Fig. 2a) is closed as the 200 Hz primary current reaches its maximum and this results in zero crossing. Figure 6 a) shows a quarter wave period of the simulated primary current. Figure 6 b) illustrates a magnification of the current switch with different resonance capacitor polarity. Simulations show that a better efficiency is acquired with positive charge in the resonance capacitor  $C_d$ . However, it does have some drawbacks that will be discussed further in section VI. The polarity of the charge voltage in capacitor  $C_d$  has a 10% influence on the efficiency of the circuit.

The switching frequency of the current is determined by all components included in the circuit. The coupling factor  $k$  of the transformer influences the resonance frequency most. The frequency dependence of the resonance

peak can be analyzed by sweeping of the coupling [11]. The parameter sweep shows that the resonance frequency changes much as the coupling factor is changed. The partly ideal circuit presented in Fig. 2 has lower resistance values than the non-ideal circuit tested in section IV.

### 3.2 Coaxial transformer

Coaxial transformers are designed using a high voltage coaxial cable where the inner conductor is used as the secondary and the screen is the primary winding [1]. The transformer used in this pulse generator was FEM (Finite Element Method) analyzed magnetically in [2]. The results showed that the FEM model was accurate at low frequencies. Deviations of the inductance occurred at higher frequencies and the behaviour is explained by the use of isotropic conductors in the model. However, a measurement of the primary and secondary impedance has been made using a function generator and a power amplifier. The transformer was analyzed for two different winding ratios  $N = 1$  and  $N = 4$  respectively. Figure 7 illustrates the measured primary and secondary impedances. Measurement of the primary and secondary currents was made using Pearson current probes. Measurement with the secondary winding short-circuited is shown in Figure and the phase angle between the voltage and current is also shown.

### 3.3 Pulse forming

In order to deliver a square load voltage pulse forming can be made by replacing the secondary capacitor  $C_s$  with a Blumlein [12], [13]. Figure 9 shows the pulse generator system and it works in the same way as described in section II, however,  $S_2$  is another type of opening switch that combines vacuum interrupters and semiconductors. The secondary capacitance  $C_s$  has to be  $0.25 \mu\text{F}$  for this specific circuit in order to make the LC-resonance circuit (section B) efficient. This relative large capacitance requires a large amount of cable and therefore the vacuum interrupter/semiconductor switch was used.

The capacitance of the Blumlein that was used had a value of 20 nF and the opening switch used could handle  $\sim 200$  A and thus limiting the secondary charge voltage to 12 kV. Since the opening switch limited the maximum current to 200 A the transformer was set to a winding ratio of  $N = 2$  in the pulse forming tests. The load is connected to the screen conductor of the line  $T_2$  and the spark gap is connected to the inner conductor as shown in Fig. 9. As the secondary sinusoidal charge voltage reaches its first maximum, the spark gap closes. A square load voltage is formed in the load.

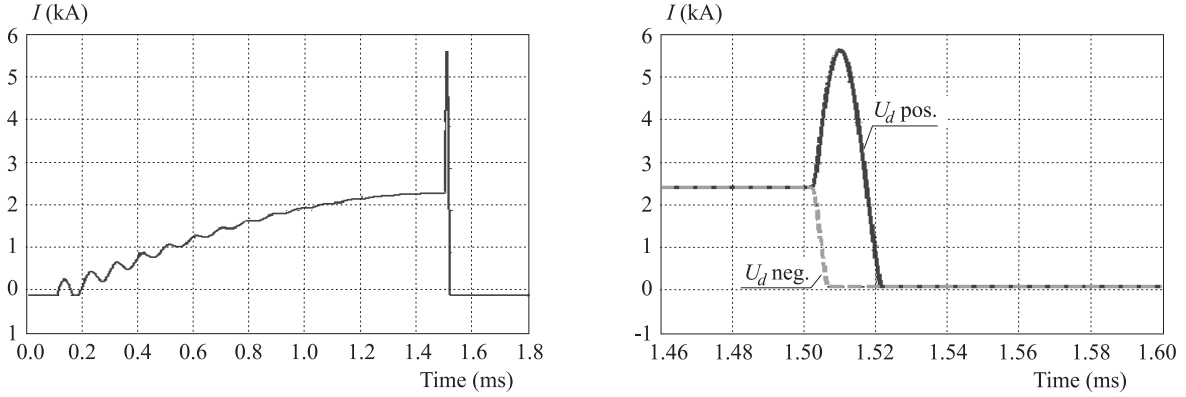


**Fig. 6.** a) The slow 200 Hz sinusoidal current receives a new 25 kHz frequency as the resonance circuit is connected, the resonance capacitor  $C_d$  is positively charged. b) Simulated primary current with positive and negative charge voltage in capacitor  $C_d$ .

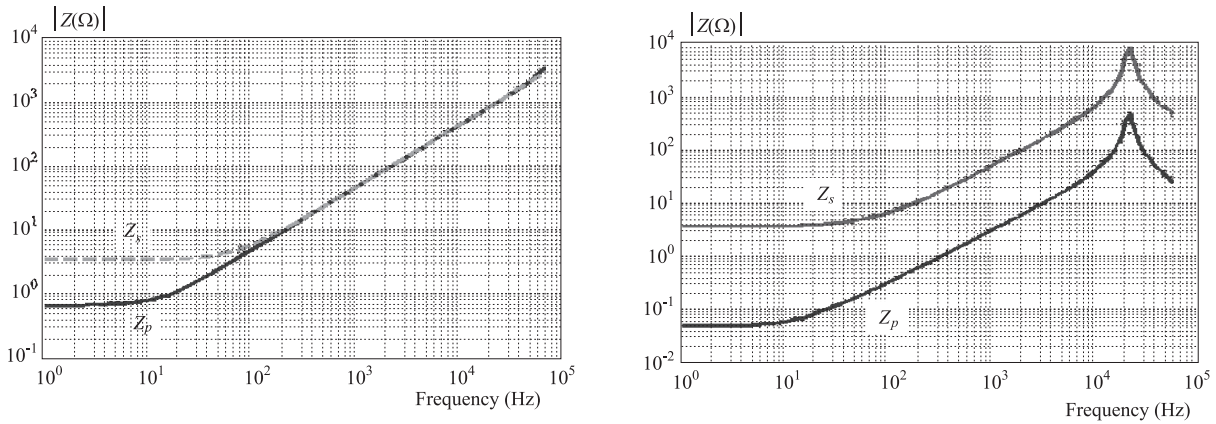


**Fig. 7.** Measured impedance with winding ratio  $N = 1$  (left) and  $N = 4$  right. The resonance peak should appear at  $\sim 100$  kHz for  $N = 1$ , however, measurement difficulties were encountered above 60 kHz.

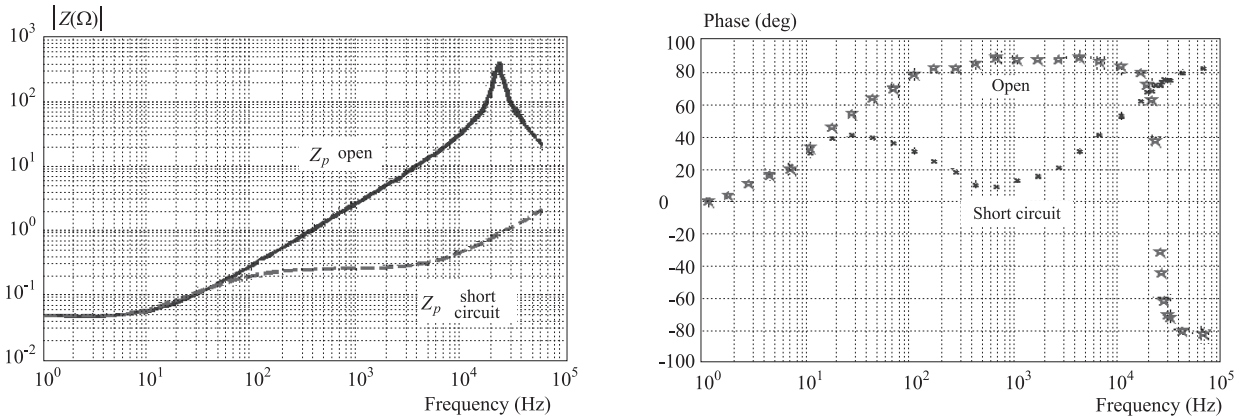


**Fig. 8.** Measured primary impedance with open and short-circuited secondary winding with winding ratio  $N = 4$  (left), the phase is shown to the right.

## 4 HIGH VOLTAGE RESULTS

### 4.1 Switching current

The high voltage measurements were made with a  $0.25 \mu\text{F}$  high voltage capacitor  $C_s$  mounted on the secondary winding of the transformer. The high voltage capacitor should be replaced with a Blumlein in order to produce square pulse shapes but the relatively high ca-

pacitance requires a large amount of cable. The voltages and currents were recorded with Tektronix 430 oscilloscopes (100 Ms/s). The primary current was measured with Pearson probes (model 101, rise time 100 ns) and the primary voltage was measured with a (Tektronix P6015 A, 20 kVDC). The measurement on the secondary side of the transformer was made with a high voltage probe (Ross Eng. Corp. Model VMP120, 120 kVDC). Figure 10 shows the results from a test with a primary

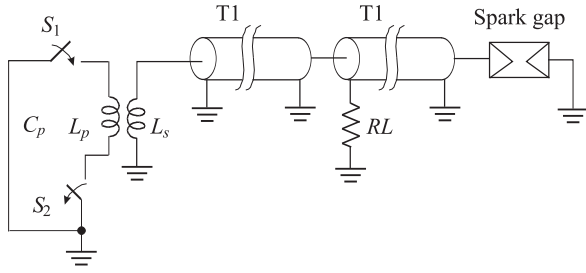


Fig. 9. The secondary capacitor  $C_s$  (shown in Fig. 2) is replaced with a pulse forming Blumlein.

current peaking at 1.8 kA and the resonance capacitor  $C_d$  was charged negative. The energy in the pre-charged resonance capacitor  $C_d$  and inductor  $L_d$  becomes equal as the current reach its maximum ( $L_d \sim 80$  J at 1.8 kA), usually the capacitor have to contain slightly more energy due to resistive losses ( $C_d \sim 90$  J at 6 kV). Simulations from a non-ideal circuit model are included next to the measured data.

A typical test as illustrated in Figs. 10 and 11 have a primary capacitor bank energy of 1440 J (at 1.2 kV) of which 1.2 kJ discharges into the transformer and 240 J is left after switching. The resonance capacitor contains a energy of 90 J at 6 kV. The secondary load capacitor is charged to 450 J at 60 kV as the current is switched off. Losses occur in the vacuum interrupters  $\sim 75$  J (assuming 50 V forward arc voltage at 1 kA for 1.5 ms). The resonance inductor  $L_d$  have an energy of 80 J at switching which will be lost and the rest is resistive losses  $\sim 600$  J. The efficiency of this test circuit is  $\sim 40\%$ , however, the efficiency can be improved by using larger conductor cross-section areas.

### 4.2 Blumlein pulse forming

The Blumlein pulse forming was made using two 50 m coaxial transmission lines. The transmission lines  $T_1$  and  $T_2$  illustrated in Fig. 9 were both wound as solenoids. The total capacitance for the coaxial cable was 20 nF. The resonance circuit  $L_d$  and  $C_d$  in the opening switch  $S_2$  loses some of its efficiency because of the small secondary capacitance. Many parallel coaxial cables are needed to achieve  $0.25 \mu\text{F}$  corresponding to the high voltage capacitor. Therefore the Blumlein tests were made using the switch described in section 3.3. The load was a water/NaCl mixture in order to reduce inductance. The load current was measured with a Pearson current probe (model 2878, rise time 5 ns) and the voltage was measured with a (Tektronix P6015 A, 20 kVDC). The spark gap shown in Fig. 9 has two copper spheres with radius 5 mm and gap distance 4 mm. The Blumlein was tested using three different load setups. The coaxial cable used in the Blumlein has the calculated characteristic impedance of  $30 \Omega$  and is calculated from measurements on the cable. The total capacitance of 20 nF stores 1.44 J at 12 kV. The energy discharged into the main pulse is 1.35 Joule, which makes an efficiency of 90 to 95% considering capacitance calculation errors *etc.* Figure 12 shows the measured load power with three types of loads.

### 5 COMMENTS

Care should be taken to have a proper shield outside the vacuum interrupters because harmful X-rays may be generated [17]. X-ray radiation may be generated if electrical breakdown occurs in the vacuum interrupters due to mismatched mechanical timing of the movable contact [18]. The rise time for the load voltage on the Blumlein is strongly dependent of the closing time for the spark gap. The electric circuit model for the opening switch should be complemented with the deionization dependence of the

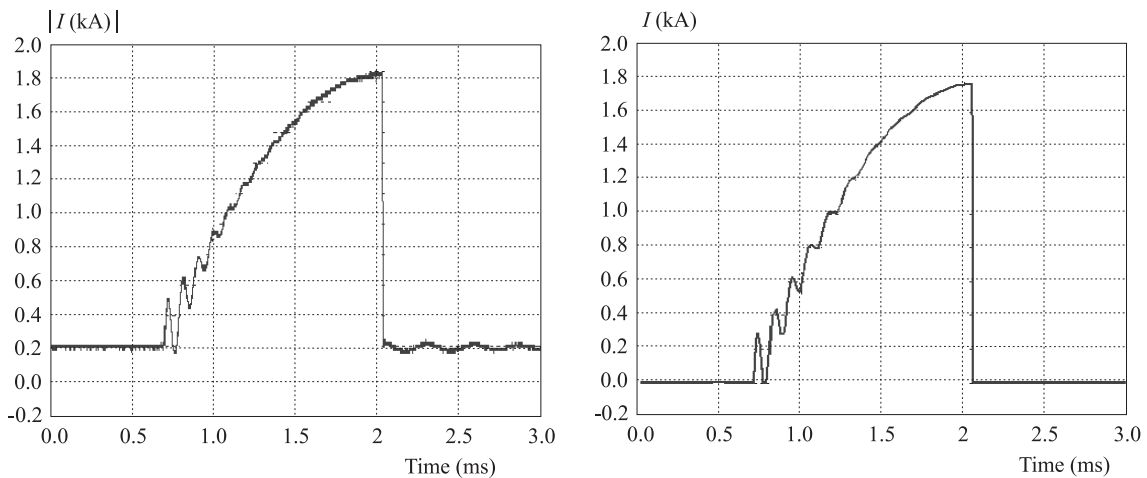
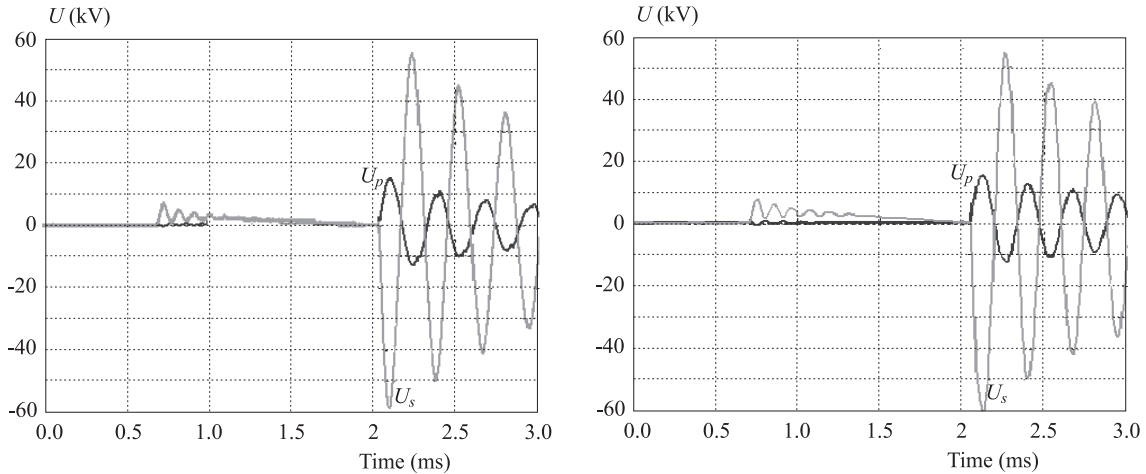
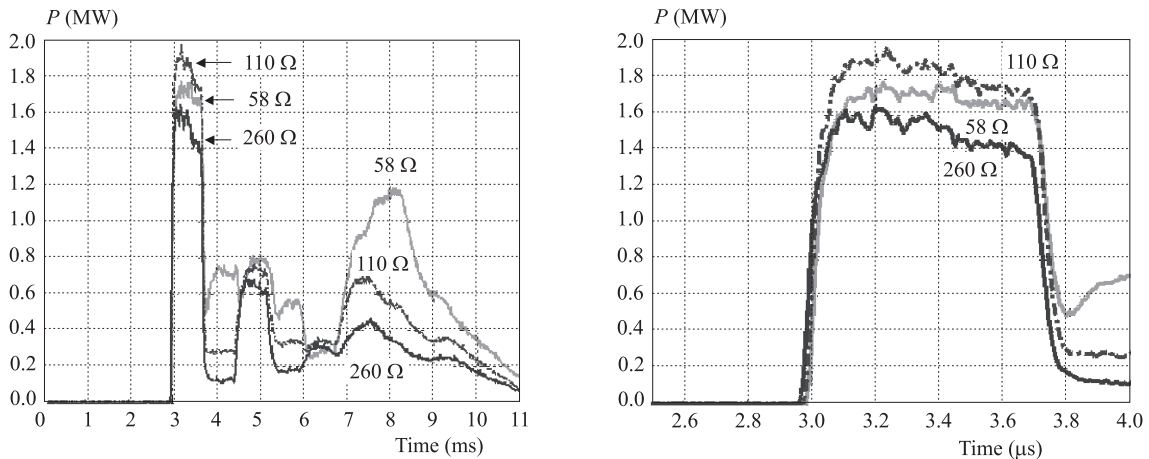


Fig. 10. The measured (left) and simulated current (right) through the primary winding with negative charge in the resonance capacitor  $C_d$ .



**Fig. 11.** The measured (left) and simulated (right) primary and secondary voltage with negative charge voltage in the resonance capacitor  $C_d$ .



**Fig. 12.** Power into varying loads with a voltage rise time of  $\sim 40$  ns and pulse length of 700 ns using  $2 \times 50$  m Blumlein.

vacuum interrupters. The spark gap shown in Fig. 9 may be moved to the secondary side of the transformer and connected directly to ground. The load voltage is reversed as the spark gap is located in this new position. Alternating load voltage may be achieved if spark gaps are used at both places. The load power is calculated using [16] and the power is peaking at the load resistance  $110 \Omega$ . Calculations according to [12] predicts a power peak at  $60 \Omega$ . A pulse length of 500 ns is achieved assuming a relative dielectric constant of cross-linked polyethylene of 2.3, however, we measure 700 ns.

Triggered vacuum interrupters should be used in order to remove the mechanics. Triggered vacuum interrupter contacts are always open and therefore the switch  $S_1$  can be removed and switch  $S_2$  works as a closing and opening switch. This enables a higher repetition rate but another trigger circuit for the vacuum interrupters are necessary.

## 6 CONCLUSIONS

The hybrid switch used in this pulse generator combines the durability of the vacuum interrupters and the

strong resonance of the LC-circuit. Combination of the two devices has proven to switch 1.8 kA. The switching of the current using positive compared to negative potential in the resonance capacitor  $C_d$  has proven to increase the overall efficiency of the generator. Positive charge in the resonance capacitor  $C_d$  gives a superimposed current as shown in Fig. 6 resulting in an inverted initial potential on the secondary side of the transformer. Measurement of the transformers impedance show that the coupling is very high for this type of transformer, as shown in Fig. 8 where the primary impedance is below  $1 \Omega$  up to 25 kHz with the secondary winding short-circuited. The pulse forming Blumlein consists of  $2 \times 50$  m coaxial cable with solenoid windings. This type of winding is preferred when compactness is desired. By placing two spark-gaps, *ie* one additional directly on the secondary side of the transformer opens the possibility to alternate the load voltage using constant polarity of the charge voltage. Considering the full-scale generator the hybrid switch should manage to switch off 3.3 kA, the coaxial transformer for 125 kV primary voltage is a challenge to design, the secondary 500 kV will constitute a challenge at the cable joints between the transformer and the Blumlein.

## Acknowledgement

The authors would like to thank the The Swedish Materiel Administration (FMV) and Swedish Defence Research Centre (FOI, Grindsjön) for their financial support. Draka Kabel is also greatly acknowledged for their high voltage cable support.

## REFERENCES

- [1] LINDBLOM, A.—APPELGREN, P.—LARSSON, A.—NYHOLM, S. E.—ISBERG, J.—BERNHOF, H.: Pulsed Power Transmission Line Transformer Based on Modern Cable Technology, *IEEE Transactions on Plasma Science* **31** No. 6 (December 2003), 1337–1343.
- [2] LINDBLOM, A.—ISBERG, J.—BERNHOF, H.: Calculating the Coupling Factor for a Multilayer Coaxial Transformer with Air-Core, *IEEE Transactions on Magnetics* **40** No. 5 (september 2004).
- [3] LEIJON, M.—DAHLGREN, M.—WALFRIDSSON, L.—LIMING—JAKSTS, A.: A Recent Development in the Electrical Insulation Systems of Generators and Transformers, *IEEE Electrical Insulation Magazine* **17** No. 3 (May-June 2001), 10–15.
- [4] MURATA, Y.—KATAKAI, S.—KANAOA, M.: Impulse Breakdown Superposed on ac Voltage in XLPE Cable Insulation, *IEEE Transactions on Dielectrics and Electrical Insulation* **3** (1996), 361.
- [5] LEIJON, M.: Powerformer — a Radically New Rotating Machine, *ABB Review* **2** (1998), 21–26.
- [6] LEIJON, M.—ANDERSSON, T.: High and Dry [Dryformer Power Transformer], *IEE Review* **46** No. 4 (July 2000), 9–15.
- [7] JOHNSON, D.—BARBER, J.—LAQUER, H.: Commutating Direct Current out of a Vacuum Interrupter with a GTO Thyristor, *Magnetics, IEEE Transactions on* **22** No. 6 (Nov 1986), 1552–1557.
- [8] van DIJK, E.—van GELDER, P.: 100 kA Test Results of the 1 MA Resonant Series Counterpulse Opening Switch System, Pulsed Power Conference, 1995. Digest of Technical Papers. Tenth IEEE International, Vol. 2, 3-6 July 1995, pp 1303–1308.
- [9] CLEMENTS, N. D.—JOHNSON, D. E.: Opening Switches for a 5 MJ, 1 MA Energy Storage Transformer, *Magnetics, IEEE Transactions on* **27** No. 1 (Jan 1991), 421–425.
- [10] HOLMBERG, P.—LEIJON, M.—WASS, T.: A Wideband Lumped Circuit Model of Eddy Current Losses in a Coil with a Coaxial Insulation System and a Stranded Conductor, *Power Delivery, IEEE Transactions on* **18** No. 1 (Jan 2003), 50–60.
- [11] P-spice, Circuit Analysis Program Version 9.2.3. Cadence Design Systems, Inc.
- [12] BAKHAREV, M. G.—GRISHANOV, B. I.—PODGORNY, F. V.: High Voltage Short Pulses Generator, Particle Accelerator Conference, 2001. PAC 2001. Proceedings of the 2001, Vol. 5, 18–22 June 2001 pp. 3765–3767.
- [13] DAVANLOO, F.—KORIO, J. L.—BOROVINA, D. L.—KRAUSE, R. K.—COLLINS, C. B.—AGEE, F. J.—HULL, J. H.—KINGSLEY, L. E.: Stacked Blumlein Pulse Generators, *Power Modulator Symposium, 1996. Twenty-Second International*, 25–27 June 1996, pp. 181–185.
- [14] POZAR, D. M.: *Microwave Engineering*, 2nd ed., John Wiley & Sons, 1998.
- [15] FUGEL, T.—KOENIG, D.: Peculiarities of the Switching Performance of Two 24 kV-Vacuum Interrupters in Series, Discharges and Electrical Insulation in Vacuum, 2000. Proceedings. ISDEIV. XIXth International Symposium on, Vol. 2, 18–22 Sept. 2000, pp. 411–414.
- [16] Matlab, The Language of Technical Computing Version 6.1.0.450 Release 12.1.
- [17] WALCZAK, K.: Method for Vacuum State Evaluation Based on Analysis of Dynamics Changes of Electron Field Emission Current and X-radiation in Time, Discharges and Electrical Insulation in Vacuum, 2002. 20th International Symposium on, 1–5 July 2002 pp. 231–234.
- [18] WALCZAK, K.—JANISZEWSKI, J.—MOSCICKA-GRZE-SIAK, H.: Evaluation of Internal Pressure of Vacuum Interrupters Based on Dynamics Changes of Electron Field Emission Current and X-Radiation, *High Voltage Engineering, 1999. Eleventh International Symposium on (Conf. Publ. No. 467)*, Vol. 5, 23–27 Aug. 1999 pp. 192–195.

Received 14 March 2006

**Adam Lindblom** was born in Kalix, Sweden, in 1973. This author became a student Member (M) of IEEE in 2005. He received the BSc degree in mechanical engineering from Umeå University, Umeå, Sweden, in 1998 and the MSc degree in engineering physics from Luleå University of Technology, Luleå, Sweden, in 2003. He received his PhD degree in Electricity at Uppsala University, Uppsala, Sweden in 2006. His research is mainly within electromagnetic fields and pulsed power.

**Jan Isberg** was born in Stockholm, Sweden, in 1964. He received the MSc degree in physics in 1987 and the PhD degree in theoretical particle physics and quantum field theory with emphasis mainly on string theory and supersymmetry in 1992, both from Stockholm University. He held a postdoctoral position in the Department of Mathematics at Kings College, London, UK, during 1993-1994. In 1995, he joined ABB Corporate Research, Västerås, Sweden, where he worked in the area of electrotechnology, in particular research on single crystal diamond as a wide bandgap semiconductor. In 2004, he was appointed Associate Professor at Uppsala University, Uppsala, Sweden. His current research interests include pulsed power and diamond semiconductor physics.

**Hans Bernhoff** received the PhD degree (focusing on the characterization and synthesis of high temperature superconductors) from the Royal Institute of Technology, Stockholm, Sweden, in 1992. He then held a Postdoctoral position with the IBM Research Laboratory, Rueschlikon, Switzerland. In 1993, he joined ABB Corporate Research, Västerås, Sweden, where he was a Project Leader for several innovative projects in the area of electrotechnology, in particular research on single crystal diamond as a wide band gap semiconductor. In 2001, he became an Associate Professor at Uppsala University, Uppsala, Sweden, where he has focussed his research and teaching in the area of renewable energy systems: wave power, wind power and energy storage.

**Mats Leijon** received his PhD in 1987 from Chalmers University of Technology, Gothenburg, Sweden. From 1993 to 2000, he was head of the department for High Voltage Electromagnetic Systems at ABB Corporate Research, Västerås, Sweden. In 2000 he became Professor of Electricity at Uppsala University, Uppsala, Sweden. Prof Leijon received the Chalmers award John Ericsson medal in 1984, the Porjus International Hydro Power Prize in 1998, the Royal University of Technology Grand Prize in 1998, the Finnish academy of science Walter Alstrom prize in 1999, the 2000 Chalmers Gustav Dahlen medal He both received the Grand Energy Prize in Sweden and the Polhem Prize in 2001 as well as the Thureus Prize 2003. He is a member of IEEE, IEE, WEC and Cigre as well as the Swedish Royal Academy of Engineering Science.